JP3J.9 **CONVECTIVE EVOLUTION IN ALONG–LINE SHEAR**

Matthew D. Parker*
North Carolina State University, Raleigh, North Carolina

1. INTRODUCTION

Convective lines in environments with line–parallel shear seem to have received relatively little attention in the literature. This may be because such systems cannot be reproduced in 2D and periodic–3D numerical simulations, which have heretofore been widely used in studies of linear mesoscale convective systems (MCSs). The present study considers some of the preferred structures that occur in environments with line–parallel vertical wind shear. Such systems may be frequently implicated in flash flooding because they entail both the along–line movement of hydrometeors and backbuilding convective development (Schumacher and Johnson, 2005).

2. METHOD

This work incorporated 3D simulations using version 5.1.0 of the Advanced Regional Prediction System (ARPS), a fully compressible nonhydrostatic model (Xue et al., 2000, etc.). In order to explicitly simulate convective clouds on the 600x600x20 km domain, the simulations had horizontal grid spacings of 1 km, with an averaged vertical grid spacing of 400 m, ranging from 200 m in the lowest 2 km of the domain to 625 m in the stratosphere. The basic model configuration was outlined by Parker (2004), and generally conformed to that used by Parker and Johnson (2004); please contact the author for more detail.

The initial thermodynamic sounding was the idealized Parker and Johnson (2004) midlatitude MCS sounding, using a simple wind profile containing both line–parallel and line–perpendicular vertical wind shear. Specifically, the u–wind (line–perpendicular) wind component linearly increased by 12 m s^{-1} between 0 and 3 km AGL, and the v–wind (line–parallel) wind component linearly increased by 25 m s^{-1} between 3 and 10 km AGL. Both components were adjusted to keep the convection centered within the domain. Convection was initiated artificially in a variety of patterns, each designed to provide the correct initial orientation of convection with respect to the vertical wind profile.

In an ongoing study of *convective lines with parallel stratiform (PS) precipitation* (for definition, see Parker and Johnson, 2000), numerous other wind profiles have been tested as a part of a sensitivity experiment. However, those results are not reported here; the present focus is on the unique behaviors of convection that develops in an environment with line–parallel vertical wind shear. This purpose is served well by the idealized environment described above.

3. BASIC EVOLUTION

With an initial linear trigger, a simulated linear convective system evolves, developing a line–parallel precipitation region (Fig. 1a) before eventually beginning to produce significant line–trailing precipitation (Fig. 1b). The convective line exhibits both leftward[1] along–line advection of hydrometeors in the anvil and rightward backbuilding. Significant along–line flow exists within its anvil precipitation region, but this along–line flow is minimized within the axis of the convective line (Fig. 2).

To explain these features, Parker (2004) discussed a basic framework and proposed a means of interpreting the accelerations experienced by air parcels within the simulated system. In short, the lower tropospheric line-perpendicular vertical wind shear is important in that is provides for reasonably upright, intense convective cells along the convective line, much as Rotunno et al. (1988) originally envisioned. The line–parallel vertical wind shear accounts for dynamical downshear pressure gradient accelerations of updraft parcels, which then gives rise to the along–line currents in the anvil regions. This along–line flow in turn leads to the development of a line–parallel precipitation region.

However, the along–line flow is minimized within the convective line's axis, because the dynamic pressure maxima associated with other cells (farther down the line) interrupt the flow stream. These pressure max-

* *Corresponding author address:* Matthew D. Parker, Department of Marine, Earth, & Atmospheric Sciences, North Carolina State University, Campus Box 8208, Raleigh, NC 27695–8208. E-mail: mdparker@ncsu.edu

[1] *Leftward* means: "to the left, with respect to the line's leading, or inflow, side." In Fig. 1, for example, "leftward" is toward the north, and "rightward" is toward the south.

ima effectively divert most air parcels into the line–leading and trailing anvils. However, the storm–relative along–line flow within the system also renders a tilted mesoscale buoyancy field within the mature convective systems (Fig. 3), associated with which is an along–line pressure gradient acceleration, much as LeMone (1983) originally envisioned on the rear side of convective lines with trailing anvils. In the present case, the along–line buoyant pressure gradient acceleration within the line–leading and line–trailing anvils slowly restores the along–line velocities of convection–processed air parcels, thereby reinforcing the along–line transports.

In time, as the surface cold pool strengthens, the convective updrafts acquire rearward tilt and air parcels begin to leave the convective region with significant front–to–rear momentum. This leads to the development of the line–trailing precipitation region (e.g., Fig. 1b). Such systems, possessing both line–parallel and trailing precipitation, bear great resemblance to the asymmetric MCSs documented by Houze et al. (1990) and others. These asymmetric structures have often been attributed to the cumulative impacts of coriolis accelerations, or to the climatological distribution of high–θ_e air in the central United States. However, neither of these explanations can be applied to the present idealized simulations, such that the behavior must be attributed to the wind profile. It appears that line–parallel shear, as in the present simulations, is sufficiently common in nature to account for many MCSs' observed evolution toward asymmetry, much as was suggested by Hilgendorf and Johnson (1998).

The preceding evolutionary features were noted and discussed previously by Parker (2004). Other key features of organized convection in along–line shear, and their causes and effects, are addressed in the remainder of this abstract.

4. ALONG–LINE HYDROMETEOR TRANSPORTS AND IMPACTS

The fact that the along–line flow in the simulated systems is maximized within the line–leading and trailing anvil regions (Fig. 2), rather than within the core of maximal hydrometeor content, seems to be consistent with observations (contact the author for more information). This raises the interesting question of whether the along–line water fluxes that lead to the developing line–parallel precipitation are most dependent upon the high water content of the heavy convective cores or upon the strong along–line flow nearby, within the region of lower water content.

Below 5 km AGL in the present simulation, the along–line fluxes are almost entirely rightward (with respect to the system's inflow side; Fig. 4), meaning that water transports in the lower–to–middle troposphere do not account for any along–line advection into the line–parallel precipitation region seen in Fig. 1. However, these rightward transports do help to account for the rightward expansion of the convective line in a storm–relative sense. As lower tropospheric hydrometeors are advected southward along the line in the simulations, they contribute to evaporative chilling that develops and reinforces the cold pool on the line's right–hand side; this appears to play a role in the backbuilding process.

In the middle and upper troposphere, the along–line water fluxes are nearly zero within the axis of maximum hydrometeor content, and are significantly leftward only in the leading and trailing anvils between roughly 5 and 12 km AGL (Fig. 4). The input of hydrometeors into the leading and trailing anvils occurs primarily between 8 and 11 km AGL, owing to forward and rearward flows that exit the convective region (e.g., Fig. 2). Beneath 8 km AGL and within 5 km on either side of the convective line, there is a narrow zone in which these hydrometeors fall into the relatively undisturbed along–line environmental flow that exists beneath the main anvils between roughly 6 and 7 km AGL (e.g., Fig. 2). The small–scale maxima in the along–line fluxes (Fig. 4), which fall between 6 and 8 km AGL, are attributable to the leftward (northward) transport of this falling precipitation by the environmental flow. However, the lion's share of the along–line fluxes that lead to the line–parallel precipitation region occur within the convection–processed cloudy air throughout the remainder of the leading and trailing anvils, rather than in the somewhat shallow belt of environmental along–line flow.

Perhaps one of the most unique aspects of MCSs in along–line shear is that their upper–level along–line flow fields advect hydrometeors downstream immediately above the outflow boundary. As a result, newly developing convective updrafts may be seeded by hydrometeors that were produced by other cells farther up the line (i.e. to the right). Idealized trajectories for the snow, graupel, and rain hydrometeor categories are depicted in Fig. 5. The overall picture is of rain and graupel particles that fall out very close to where they were generated; rain exists only in the lower troposphere, and graupel has a relatively large terminal velocity. However, snow has a fairly small fallspeed and is primarily found aloft in regions where the line–parallel flow is significant. As a result, it can be advected large distances along the line (Fig. 5).

First, this underscores the fact that the advection of snow is of prime importance to the development of the line–parallel precipitation region in the simulations. Of additional interest, however, is the ability of these snow particles to fall into newly developing updrafts (Fig. 5, thick gray trajectories).

The along–line advection of hydrometeors does not overwhelm developing updrafts farther down the line because most of the along–line transport comprises snow. Given snow's low density and fallspeed, drag from the particles that fall into active updrafts does not hinder their development much. However, introduction of already–grown snow into a fresh updraft clearly can accelerate the production of precipitation (the "seeder–feeder" mechanism) through both vapor deposition and accretion.

Indeed, a seeded updraft will more rapidly experience the reversal to negative buoyancy due to hydrometeor loading and chilling from melting. A sensitivity test compared the development of an isolated updraft (from a single warm bubble) in a pristine environment to development in an environment with 1.4 g kg^{-1} of snow[2] falling from between 6 and 11.5 km AGL. The presence of the seeding snow accelerated the onset of surface precipitation by about 1 minute, and increased the peak surface rainfall rate by roughly 14%. As a result, the snow–seeded experiment produced a much stronger surface outflow than the pristine updraft experiment: after 40 minutes, the cold pool was 0.7 K colder (–7.5 K vs –6.8 K), very slightly larger, and had a surface pressure perturbation that was 34% greater (1.45 hPa vs. 1.08 hPa) due to its increased depth. It is in this way that the along–line motion of hydrometeors can lead to rapid intensification of the surface cold pool. This explains why many such systems evolve from producing line–parallel to line–trailing precipitation, as mentioned above and frequently observed by Parker and Johnson (2000).

5. BACKBUILDING MECHANISM

As has been mentioned, another critical component of organized convection in along–line shear is that the convection continually backbuilds toward the system's right. In part this is because a general northerly flow prevails immediately behind the gust front in the simulated systems (Fig. 2). As described earlier, this entails the rightward (southward) advection of hydrometeors in the lower troposphere, which may make the system's right flank a preferred location for evaporative chilling. It also entails a general rightward expansion of the surface cold pool through advection of the outflow air.

In addition, a closer analysis reveals that each individual downdraft that contributes to the surface cold pool generally also entails a northerly surge in wind within the cold pool. Numerous such surges, with attendant gust fronts, are evident throughout the outflow at any given time (Fig. 6a). Indeed, it is these surges that lead to the scalloped shape of the main outflow boundary (Fig. 6a).

Dynamically, the northerly flow associated with each downdraft pulse can be attributed to the along–line vertical wind shear. Downdrafts in the presence of southerly along–line shear experience southward along–line accelerations, leading to the structures seen in Fig. 6a. This process works best when there is along–line shear extending all the way to the surface, but the generation of northerly outflow surges is still significant even in the present wind profile (with no along–line shear below 3 km AGL). The intersections between these northerly gust fronts and the main outflow boundary are regions that favor new development because the lifting associated with the two features is superposed. Upward velocities are maximized above the northerly gust fronts (Fig. 6b). As well, the cold pool is somewhat deeper in these areas due to convergence (Fig. 6b), and this in turn provides for deeper lifting along the main north–south outflow boundary.

Animations reveal that all of the northerly gust fronts move southward within the cold pool. As a result, the favored regions of new convective development move southward in time. In other words, a new cell "n", will most likely occur to the south of its immediate predecessor, "$n-1$", in a storm-relative sense, because it is most likely to develop along the intersection of the main outflow boundary and the northerly gust front of "$n-1$". This convective–scale mechanism is the explanation for why along–line vertical wind shear entails backbuilding.

6. THREE–DIMENSIONALITY AND LINE–END EFFECTS

It was suggested above (see also Parker, 2004) that the along–line shape of the buoyancy field entails line–parallel pressure gradient accelerations in the near–line anvil regions. In this respect, line–end effects appear to have a significant impact on the evolution of organized convection in along–line shear. This claim can be readily tested by rerunning the control simulation with a quasi–2D (Q2D), y–periodic model configuration.

After 6 h of simulation, the fully 3D control run had produced the aforementioned asymmetric hybrid system (Fig. 1b); in contrast, the Q2D control simulation produced almost no trailing precipitation by t=6 h (not shown). The generation of a trailing precipitation region is favored in the 3D control simulations because convection can occur along the flanks of the surface cold pool, where the outflow boundary–perpendicular component of the vertical wind shear is somewhat weaker. In these locales, air will experience comparatively small rear–to–fore line–perpendicular accelerations, and will tend to exit the convective region and move over the cold pool. This, in turn, entails the development of trailing precip-

[2]This is in the 70th percentile of values observed within the simulated system's anvil.

itation behind the flanks of the original convective line. In contrast, development along these non–perpendicular flanks is impossible in the Q2D configuration.

The surface cold pool is also stronger in 3D than in the Q2D control simulations (at t=3h, in 3D: θ'=–7.1 K, p'=1.46 hPa; in Q2D: θ'=–6.0 K, p'=1.15 hPa). Because the Q2D simulations are periodic, they are insulated from the dry environmental air that is present at the line ends in 3D. They therefore lack some of the evaporative chilling that is present in a finite–length line. Comparatively strengthening or weakening the surface cold pool also respectively tends to promote or dampen evolution toward the production of trailing precipitation (Rotunno et al., 1988; Parker and Johnson, 2004, etc.).

Beyond the much delayed evolution toward production of trailing precipitation, it is also important that the along–line fluxes are significantly diminished in going from 3D to the Q2D configuration. This is because air parcels in the anvil region aloft do not experience the along–line accelerations associated with the 3D buoyant pressure field. As discussed above, air parcels are generally unable to flow along the line's axis for significant distances because other cells farther down the line interrupt them. However, the along–line pressure gradient accelerations associated with the mesoscale buoyancy field provide persistent support for the along–line fluxes in the nearby anvils. This is a line–end effect, because it relies upon the mean along–line gradient in the vertical profile of buoyancy. When this effect is removed, the flow along the line's axis continues to be interrupted, and the additional lack of line–parallel accelerations in the anvil regions cannot make up for it. So, it is the along–line fluxes that render the characteristic 3D structure, and this three–dimensionality itself is important to the long–term sustenance of the along–line accelerations.

7. QUASI–SUPERCELLULAR CHARACTERISTICS

A reasonable question is whether supercell–like behaviors are observed within the simulated system, given the significant speed and directional shear of the vertical wind profile. As shown by Fig. 7, a mature updraft in the early stages of the control simulation is flanked by positive vorticity to its southeast and negative vorticity to its northwest. As a result there are dynamical pressure minima on these two sides of the updraft at midlevels. Associated with these pressure minima are upward dynamic pressure gradient accelerations, which are not colocated with the updraft. As originally discussed by Lilly (1986), they provide forcing for new updraft development on the initial updraft's flanks, and thus can cause it to split.

Later in the system's lifetime, as discussed, the surface cold pool rapidly strengthens. This seems to suppress the tendency for isolated quasi–supercellular elements and storm splitting (not shown). The cold pool's edge forces a strongly linear gust front updraft, which is therefore less amenable to the development of isolated cells. Mature updrafts during the later stages of the simulations may still exhibit flanking vortices due to tilting of environmental horizontal vorticity. However, these cells are generally well rearward of the surface outflow boundary due to the deep solenoidal circulation associated with the enhanced cold pool. As a result, although upward accelerations may occur along updrafts' flanks, these accelerations are atop the surface outflow and not properly placed to generate an updraft that will ingest environmental inflow. Therefore, storm splitting appears to become increasingly rare once the system's cold pool has intensified.

There is also some interest and concern over the degree to which the method of initiation controls the eventual organization of convection in idealized numerical simulations. In order to determine the degree of variability in convective storms that might occur in the control environment, simulations were rerun using lines of 1–5 axisymmetric warm bubbles as initial triggers, whose horizontal spacing varied between 50 and 100 km.

For one individual axisymmetric bubble in the control environment, the convective behavior was somewhat distinct. Isolated quasi–supercellular behavior occurred, with updraft–flanking vortices leading to storm splitting.

With the inclusion of any number of additional, aligned bubbles, evolution to the PS structure (e.g., Fig. 1a) occurs along very similar pathways to the original simulations that used a long, linear thermal. However, with fewer bubbles the process of upscale organization occurs more slowly because it takes time to create a reasonably large and strong surface cold pool. The deciding factor is the ability of an initial group of storms to produce a quasi–linear outflow boundary that is nearly perpendicular to the lower tropospheric vertical wind shear vector. This, in turn, establishes a persistent region of intense lower tropospheric lifting. As well, when somewhat isolated storms are initiated along lines, the upshear/upline storms may be able to seed the downshear/downline storms (much as in Section 4), hence accelerating the rate at which they produce precipitation and outflow.

When only two bubbles were included, they needed to be somewhat near one another in order to accomplish these effects. In an experiment in which the two axisymmetric bubbles were 100 km apart, short–lived, isolated storms developed because the initial storms were not close enough to interact and produce a combined cold pool. However, when the spacing of the two bubbles was reduced to 66.7 km, a combined cold pool resulted and a PS MCS developed slowly over time. When three

or more axisymmetric bubbles were used, a PS MCS developed even for spacings as great as 100 km.

8. CONCLUSIONS

Although the studied environments are initially supportive of supercells, the merging of outflows soon renders a predominant linear forcing. Thereafter, along–line flow within the system's cold pool entails backbuilding on both the mesoscale and the convective scale. As well, along–line flow in the upper troposphere within the system entails along–line hydrometeor transports, especially in the leading and trailing anvils. These behaviors lead to the archetypal structure of a convective line with parallel precipitation.

Along–line hydrometeor advection means that much of the system's precipitation falls very near its outflow boundary, and that the convective cells can seed other updrafts farther down the line. As a result, convective systems in line–parallel shear can intensify their cold pools quite rapidly. As well, in time the convective line begins to possess diminished upper tropospheric along–line flow within its axis. These factors may hasten transition toward a predominantly rearward–sloped updraft and the production of trailing precipitation.

Even in the absence of Coriolis accelerations, this kind of convective evolution in environments with line–parallel shear will lead to highly asymmetric structures, such as are commonly observed in midlatitudes. The dynamics of such systems are irreducibly 3D, which may explain why they have received inadequate attention to this point.

REFERENCES

Hilgendorf, E. R., and R. H. Johnson, 1998: A study of the evolution of mesoscale convective systems using WSR–88D data. *Wea. Forecasting*, **13**, 437–452.

Houze, R. A., Jr., B. F. Smull, and P. Dodge, 1990: Mesoscale organization of springtime rainstorms in Oklahoma. *Mon. Wea. Rev.*, **118**, 613–654.

LeMone, M. A., 1983: Momentum transport by a line of cumulonimbus. *J. Atmos. Sci.*, **51**, 281–305.

Lilly, D. K., 1986: The structure, energetics and propagation of rotating convective storms. Part I: Energy exchange with the mean flow. *J. Atmos. Sci.*, **43**, 113–125.

Parker, M. D., 2004: Simulated convective lines with parallel precipitation. Preprints, *22nd Conf. on Severe Local Storms*, Hyannis, MA, Amer. Meteor. Soc., CD–ROM, 6.3.

Parker, M. D., and R. H. Johnson, 2000: Organizational modes of midlatitude mesoscale convective systems. *Mon. Wea. Rev.*, **128**, 3413–3436.

Parker, M. D., and R. H. Johnson, 2004: Structures and dynamics of quasi–2d mesoscale convective systems. *J. Atmos. Sci.*, **61**, 545–567.

Rotunno, R., J. B. Klemp, and M. L. Weisman, 1988: A theory for strong, long–lived squall lines. *J. Atmos. Sci.*, **45**, 463–485.

Schumacher, R. S., and R. H. Johnson, 2005: Organization and environmental properties of extreme–rain–producing mesoscale convective systems. *Mon. Wea. Rev.*, **133**, 961–976.

Xue, M., K. K. Droegemeier, and V. Wong, 2000: The Advanced Regional Prediction System (ARPS) — A multi–scale nonhydrostatic atmospheric simulation and prediction model. Part I: Model dynamics and verification. *Meteor. Atmos. Phys.*, **75**, 161–193.

ACKNOWLEDGMENTS

The research reported here is supported by the National Science Foundation under Grant ATM–0349069. Most of this work was completed while the author was a member of the Department of Geosciences at the University of Nebraska–Lincoln (UNL); their support and encouragement is gratefully acknowledged. The simulations in this study were made using the Advanced Regional Prediction System (ARPS) developed by the Center for Analysis and Prediction of Storms (CAPS), University of Oklahoma. These simulations were performed using the Research Computing Facility at UNL, whose staff–members have been of great assistance.

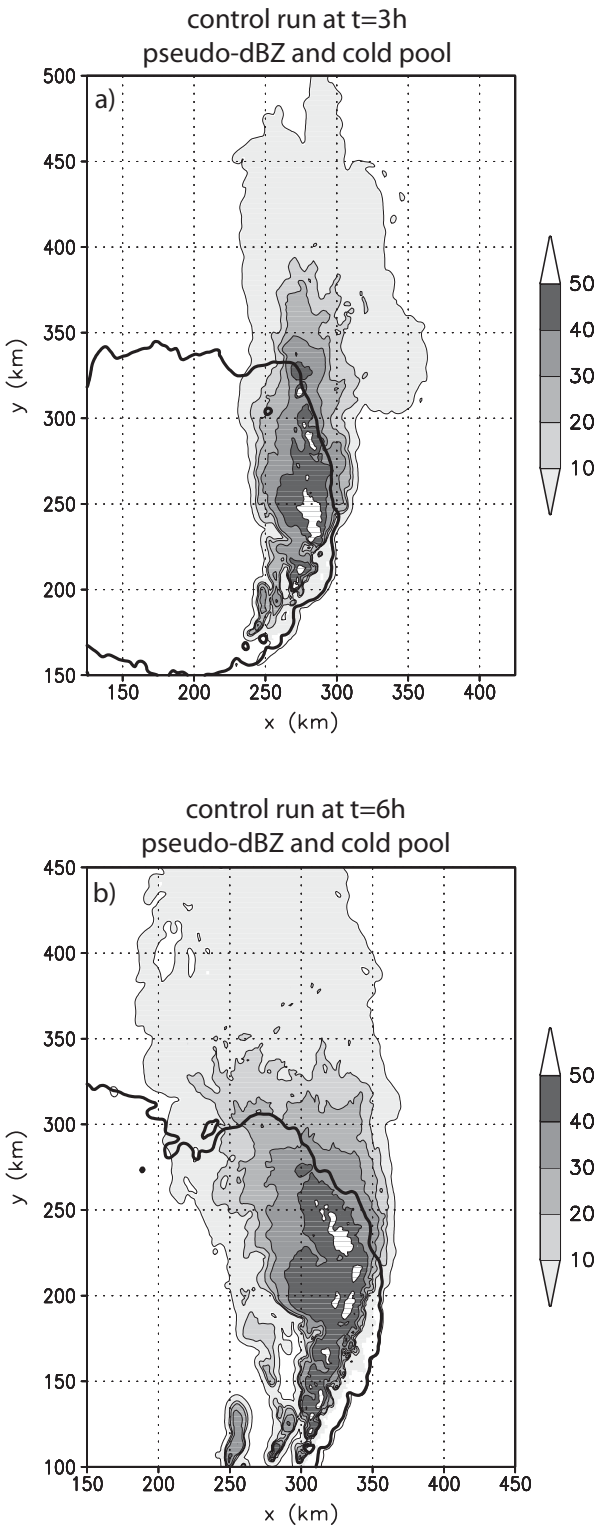

Figure 1: Plan views of vertically averaged (from z=0–10 km) radar reflectivity (simulated), shaded (dBZ), with cold pool outline indicated by thick contour (isopleth of θ'=–2K). For the control simulation (a) at t=3h, and (b) at t=6h.

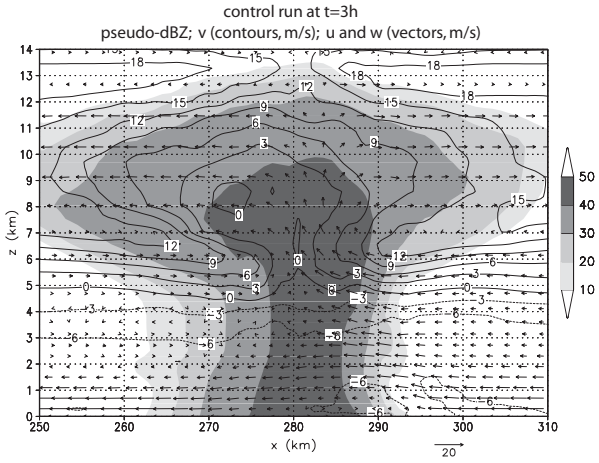

Figure 2: Vertical cross section of along–line averaged (from y=250–350 km, cf. Fig. 1) radar reflectivity (simulated), shaded, line–parallel wind (v, contoured, m/s) and line–perpendicular circulation (u and w, vectors, m/s), for the control simulation at t=3h.

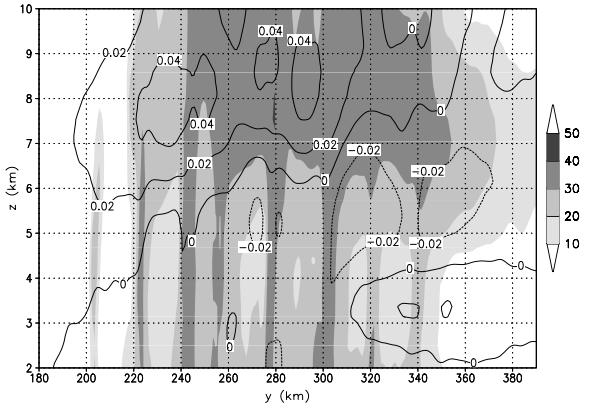

Figure 3: Line–parallel cross–section of across–line averaged fields for the control simulation at t=2h: Simulated radar reflectivity (dBZ, shaded) and buoyancy (m s^{-2}, contoured). The averages are computed over a 65 km wide area centered on the convective line.

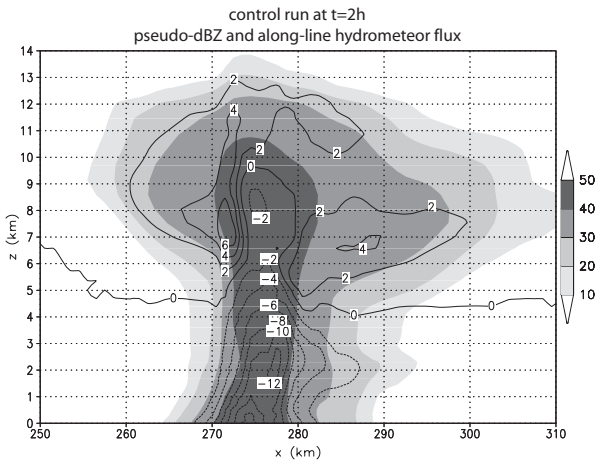

Figure 4: Vertical cross–section of along–line averaged radar reflectivity (simulated), shaded, with the along–line hydrometeor flux contoured ($\times 10^{-3}$ kg s^{-1} m^{-2}), for the control simulation at t=2h; positive values are "leftward" (into the page).

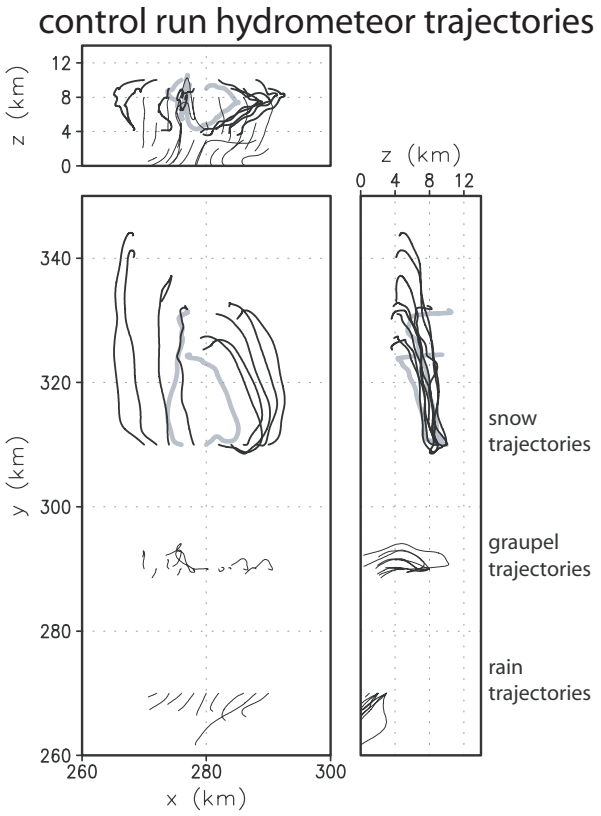

Figure 5: Projection of simulated 3D hydrometeor trajectories onto three Cartesian planes. Lower left: y vs. x plot; upper left: z vs. x plot; lower right: z vs. y plot. The trajectories shown are for rain (light weight), graupel (medium weight), and snow particles (heavy weight) from t=1:30–2:30 in the control simulation. Two snow trajectories that re–enter updrafts are shaded gray.

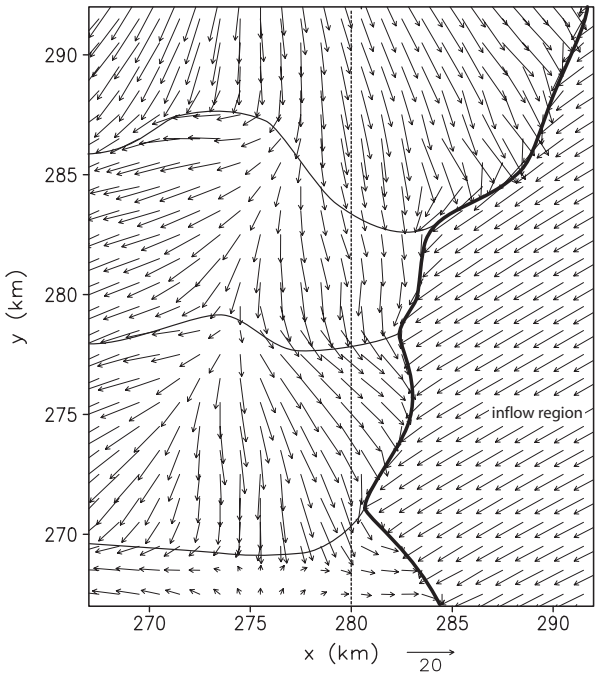

(a)

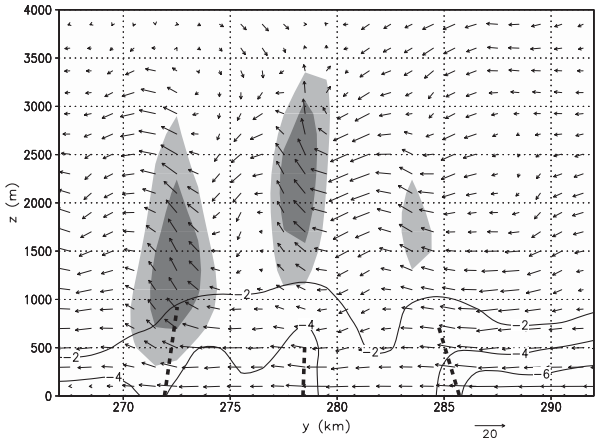

(b)

Figure 6: Depiction of northerly wind surges in the surface cold pool of the control simulation at t=2h. (a) Horizontal wind vectors at 100 m AGL: outflow boundary indicated by heavy solid curve; northerly gust fronts within cold pool indicated by thin solid curves. (b) Vertical cross–section depicting wind vectors, vertical velocity (shaded at 2.5 and 5 m s^{-1}), and temperature perturbation in the cold pool (contoured at –2, –4, and –6 K). The location of the cross–section in (b) is x=280 km, as shown by a dashed line in (a).

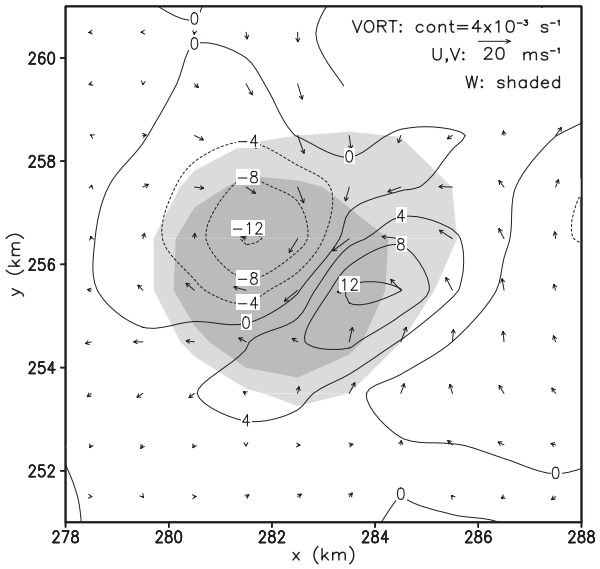

Figure 7: Fields from z=5.3 km AGL showing incipient storm split in the control simulation at t=58 min. Vertical velocity is shaded at 5 and 10 m/s, vertical vorticity is contoured (labels have units of 10^{-3} s^{-1}), and horizontal winds are shown as vectors (scaled as indicated).